SUPPLEMENT MATERIAL

DETAILED METHODS

Mice. Homozygous *myd* mice were generated from mating heterozygous mice in a colony of B6C3Fe-a/a-LARGE*myd* mice originally purchased from Jackson Laboratories. Mice homozygous for the floxed allele of the DAG1 gene were previously described(1). Transgenic mice that express cre recombinase in ventricular cardiac myocytes under control of the myosin light chain 2v regulatory region (MLC2vcre) were a kind gift from Dr. Kenneth Chien (Harvard University) (2). Mice expressing cre recombinase in smooth muscle cells under the control of the smooth muscle myosin heavy chain promoter were a kind gift from Dr. Gary Owens (University of Virginia) (3). Mice deficient for DAG1 were generated by mating male mice that were heterozygous for the cre transgene and homozyogous for the DAG1 floxed allele with females that were homozyogous for the DAG1 floxed allele, and mice were born from these crosses with normal Mendelian ratios. Analysis of several litters from crosses of MLC2vcre mice where 50% of the offspring were predicted to carry the transgene showed 42/76 mice carried the MLC2vcre transgene. Analysis of several litters from crosses of SMMHC mice where 50% of the offspring were predicted to carry the transgene showed 17/36 mice carried the SMMHCcre transgene. All comparisons were made on age and sex matched littermate mice.

Dystroglycan glycosylation, protein expression and laminin binding activity. Dystroglycan glycosylation and protein expression were analyzed using a combination of a glycosylation- sensitive dystroglycan antibody (IIH6) and dystroglycan antibodies (SHP5ADG) which recognize the core protein of α-DG, and AP83 or NCL-b-DG(Novocastra) which recognizes α-DG) as previously described (4). Briefly, tissues were homogenized in Tris buffered saline, pH 7.5 (TBS) containing 1% TX-100 using 1mL per 100mg tissue. Solubilized glycoproteins were enriched with wheat germ agglutin (WGA, Vector Laboratories) agarose beads and eluted with TBS containing 0.1% TX-100 and 0.5 M N-acetlyglucosamine. Samples were analyzed using 3-15% SDS-PAGE followed by Western blotting. Dystroglycan specific laminin binding activity was measured with blot overlay assays using purified laminin-1 as described (4). Total laminin binding activity in the glycoprotein preparations was measured using solid phase binding analysis as previously described(4). Briefly, WGA glycoproteins were diluted 1:50 in TBS and coated on Costar RIA-ELISA plates. Following washing and treatment with blocking buffer (TBS + 3% BSA + 0.1% Tween 20), plates were incubated with purified laminin-1 diluted in blocking buffer containining either 1mM $CaCl_2$ or 5mM EDTA. Bound laminin was detected by sequential application of a rabbit polyclonal anti-laminin antibody (Sigma) in blocking buffer and an anti-rabbit IgG conjugated to horseradish peroxidase (Jackson Immunochemicals). Plates were developed with 0-phenylenediamine/dihyrogen peroxide in citrate buffer, pH 5.0 and reactions were terminated with sulfuric acid. Colorimetric quantification was performed on a Biorad Benchmark Plus microplate reader.

For quantifying the expression dystrophin glycoprotein complex and dysferlin in gene targeted mice, ventricles were homogenized in 1% TX-100, total protein was quantified using DC Protein Assay (Biorad) for normalization, and samples were analyzed by 3-15% SDS PAGE and Western blots as described above. Monococlonal antibodies against β-SG and dysferlin monoclonal antibodies were obtained from Novacastra.

Morphological characterization and immunohistochemistry

Hearts were removed from anesthetized mice, atria and greater vessels were removed, blood was removed from the chamber by wicking, and the wet heart weight was obtained. For histology, mice were perfused with formalin followed by removal of the heart, paraffin embedding and sectioning. For routine histology, 4 micron sections were stained with hematoxylin and eosin. For characterization of fibrosis, sections were stained with 0.1% picrosirius red/0.1% Fast Green. For quantification of fibrotic areas, ventricular chamber cross sections sections were analyzed by ImageJ to quantify picrosirius red stained areas and normalized to the total cross sectional area of the heart. For immunofluorescence localization,

hearts were removed and frozen in liquid nitrogen-cooled isopentane. Eight micron fresh cyrosections were fixed in 3% paraformaldehyde, blocked with PBS + 3% BSA and were stained with dystroglycan antibodies diluted in blocking buffer followed by incubation with Cy3-conjugated secondary antibodies (Jackson Immunochemicals).

In vivo echocardiography. Mice were analyzed by *in vivo* echocardiography while conscious as described (5). Mice were lightly sedated with midazolam (0.15 mg SC). A 15-MHz linear-array probe was applied horizontally to the chest with the mouse held by the nape of the neck and cradled in the imager's hand. The imaging probe was coupled to a Sonos 5500 imager (Philips Medical Systems, Bothell, Wash), which generated ≈180 to 200 2-dimensional frames per second. Images were acquired in both short- and long-axis left ventricular (LV) planes. Pulse-wave Doppler tracings were measured near the ventricular aspect of the mitral valve to measure heart rate. All images were acquired and then analyzed offline with the imager blinded to mouse genotype. Endocardial and epicardial borders were traced in the short-axis plane at end diastole and end systole using custom designed software (Freeland Medical Systems, Louisville, Colo). The lengths from the left ventricular outflow tract to the endocardial apex and the epicardial apex, respectively, were measured at end diastole and end systole. Left ventricular mass, end diastolic left ventricular volume, and end-systolic left ventricular volume were calculated by the biplane area-length method(6).

RT PCR for pathological markers of cardiomyopathy. Total RNA was isolated from snap frozen heart samples using TRIzol reagent (Invitrogen), DNase treated and purified with Qiagen RNeasy Mini Kit. Only RNA samples with absorbance ratios 260/280 nm between 1.8 and 2.2 and reserved RNA integrity as checked by denaturing agarose gel electrophoresis were used for further experiments. cDNA was synthesized from 0.6 µg of total RNA using High Capacity cDNA Reverse Transcription kit (Applied Biosystems). Real-time PCR experiments were performed using SYBR Green chemistry on iCycler iQ Detection System (Biorad). Primer sets for mouse atrial natriuretic factor (NPPA) and beta-2-microglobulin (B2M) gene were designed using the Primer Express 1.5 software according to Applied Biosystems' guidelines. The primers were as follows: NPPA forward/reverse 5'-CCATATTGGAGCAAATCCTGTGT-3'/5'-CTTCTACCGGCATCTTCTCCTC-3'; B2M forward/reverse 5'-TCTTTCTGGTGCTTGTCTCACTG-3'/5'- GTTCGGCTTCCCATTCTCC-3'. For the β-myosin heavy chain gene,primers published by Gaussin et al (7) were used . B2M was selected as an endogenous reference based on literature survey (8-10). A threshold cycle (C_t) value of *B2M* and a target gene was measured at least in two independent runs, each time in triplicate. To quantify a relative change in gene expression, the comparative C_t method was used (11). All comparisons were done using unpaired two-tail unequal variance *t*-test with a significance threshold of $P<0.05$.

In vivo assessment of myocardial membrane damage. Mice with cardiac specific dystroglycan gene disruption and wild-type littermates, <5 months of age, were subjected to a single bout of 1-hour long running on a treadmill with an in-built shock grid with 5 degree inclination. Initial running speed of 7 m/min was increased every 2 minutes by 3 m/min until the maximal speed without signs of exhaustion or refusal to run (~16m/min) was achieved. Five hours before the exercise session, mice were given an i.p. injection of 0.1 mg/ g Evans blue dye in saline. Next morning after exercise completion (~18 h), hearts were removed from anesthetized animals and frozen in isopentane cooled in liquid nitrogen. A set of non-exercised mutant and wild-type mice were injected with Evans blue dye and their hearts were collected the same way as for exercised animals. Frozen heart samples were sectioned at 8 microns in a cryostat. From each heart, 4 cross-sections >250-300 microns apart were obtained. Immunostaining with anti-laminin 1 antibody (Sigma, 1:1000) and secondary antibody conjugated to Alexa 488 (Molecular probes, 1:800) was used to show cell boundaries on Evans blue treated tissue. Each slide was scored for Evans blue positive cells using an Olympus BX51 microscope (Olympus, Tokyo, Japan).

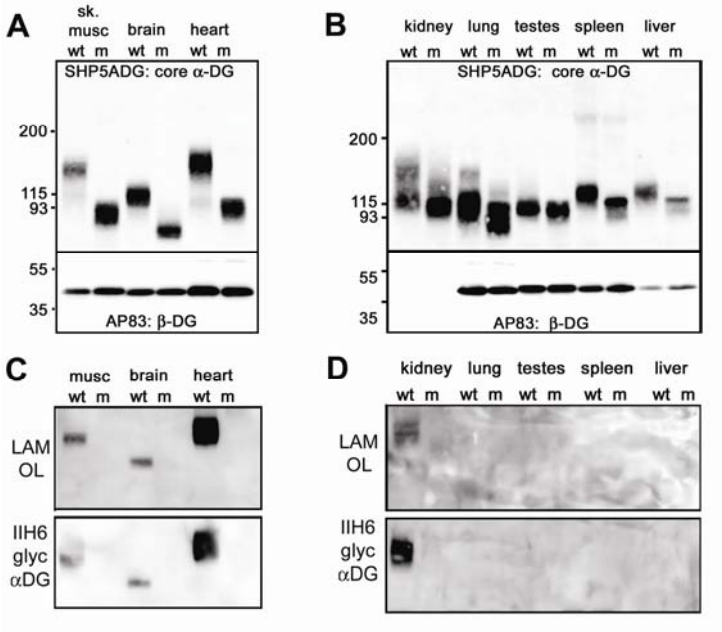

Online Figure 1. Distribution of dystroglycan glycosylation in tissues of WT and LARGE *myd* mice. In this series of experiments, WGA enriched extracts were prepared from individual tissues from WT (w) and *myd* (m) mice and the Western blots and overlay assays were performed on replicate blots shown in panels A-D. Therefore, the reactivity of the IIH6 antibody recognizing the glycosylated alpha dystroglycan (glyc. α-DG) and laminin overlay assays (LAM OL) can be compared to amount of alpha dystroglycan recognized by the core alpha dystroglycan peptide antibody (SHP5ADG) in the data series shown. Sk. Musc, hindlimb skeletal muscle, AP83 β-DG, beta-dystroglycan peptide antibody; **A and B)** Assessment of □DG protein expression in tissues of *myd* mice by Western blotting using an antibody that recognizes the core □DG protein shows dramatic changes in molecular weight are largely confined to muscle and brain tissues. **C and D)** The fully glycosylated α-DG (recognized by IIH6) and laminin binding glycoform (determined by laminin overlay assay) of α-DG are easily detected in muscle tissues, brain and kidney but not in other tissues of wild-type mice, nor in any tissues from *myd* mice. The reason for the failure to detect of beta-DG in kidney is unclear but may represent differential proteolytic cleavage of beta DG in kidney.

Supplemental Information for Online Figure 1. The characterization of the requirement for LARGE for the functional modification of dystroglycan across tissues (Figure 1, Suppemental Figure 1), suggests that loss of LARGE has the greatest impact on glycosylation in skeletal muscle, cardiac muscle, smooth muscle, and nervous system, and that it also has some impact in the kidney while other tissues are generally less affected. Notably, most of the tissues in which the apparent molecular weight of □-DG are not significantly affected by the LARGE mutation, the molecular weight α-DG is fairly low, and IIH6 reactivity and laminin binding activity are virtually not detectable. Whether these low molecular weight, non laminin binding glycoforms of α-DG have a functional role in non-muscle tissues is not clear. The molecular basis for the heterogeneity of dystroglycan glycosylation in different tissues is also not known. Even in the LARGE deficient *myd* mice, the heterogeneity of dystroglycan glycosylation in different tissues is quite pronounced (Figure 1, Supplemental Figure 1) indicating while LARGE dependent glycosylation is very important for laminin binding activity, it is not the only factor that contributes to the

tissue heterogeneity of dystroglycan glycosylation. In the mouse genome, there is a homologue for LARGE called LARGE2, that is able to glycosylate α-DG and induce laminin binding activity when overexpressed in cultured cells (12). However, our results suggest that the endogenous activity of LARGE2 in adult animals is probably insufficient because all tissues tested that showed significant amounts of highly glycosylatd dystroglycan in WT mice, show dramatic loss of dystroglycan glycosylation and function in LARGE deficient *myd* mice. *Myd* mice, which carry a large null deletion in the LARGE gene can survive to live birth and beyond. This is in stark contrast to the dystroglycan, fukutin and POMT1 knockout mice which are all embryonic lethal at E9.5(13-15). Therefore, it remains possible that LARGE2 is required, or may compensate for loss of LARGE, with respect to the dystroglycan glycosylation events that are critical during mouse development.

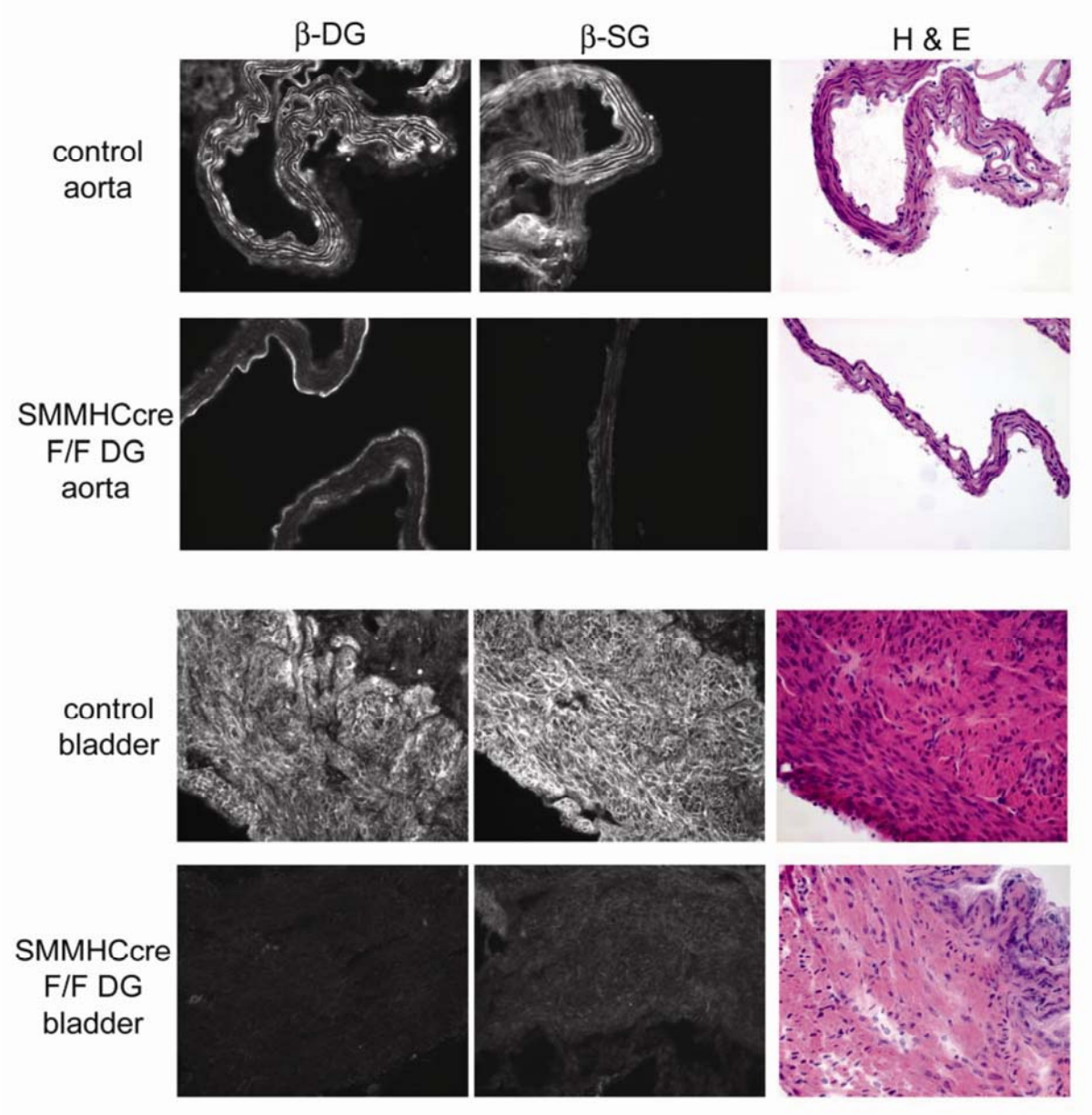

Online Figure 2. Targeted deletion of dystroglycan in smooth muscle leads to a marked reduction in sarcoglycan expression in smooth muscle. Immunostaining of β-DG and β -sarcoglycan in frozen sections of aorta and smooth muscle of SMMHCcre-L/L mice.

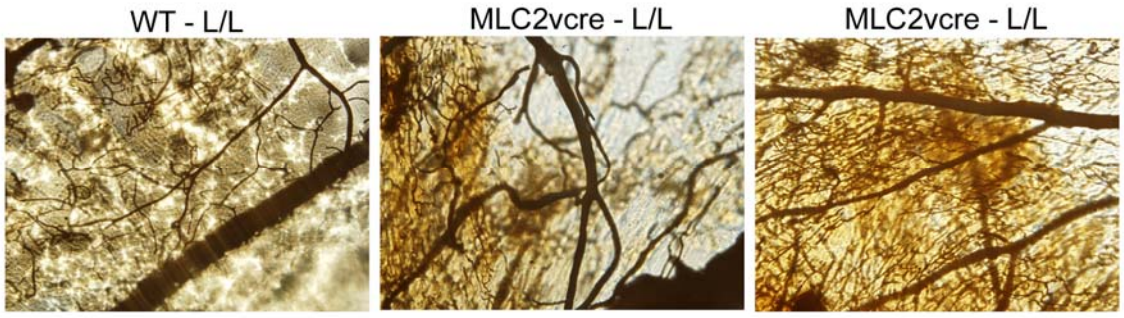

Online Figure 3. Microfil perfusion experiments at 8 months of age do not show evidence of coronary vasopasm in MLC2vcre-L/L mice compared to WT-L/L littermates.
Mice were perfused with Microfil MV-122 by cardiac puncture, and hearts were cleared with graded solutions of ethanol and methyl salicyclate as described by the manufacturer (Flowtech, Inc.) Thick sections were obtained and viewed on a Olympus BX-51 upright microscope.

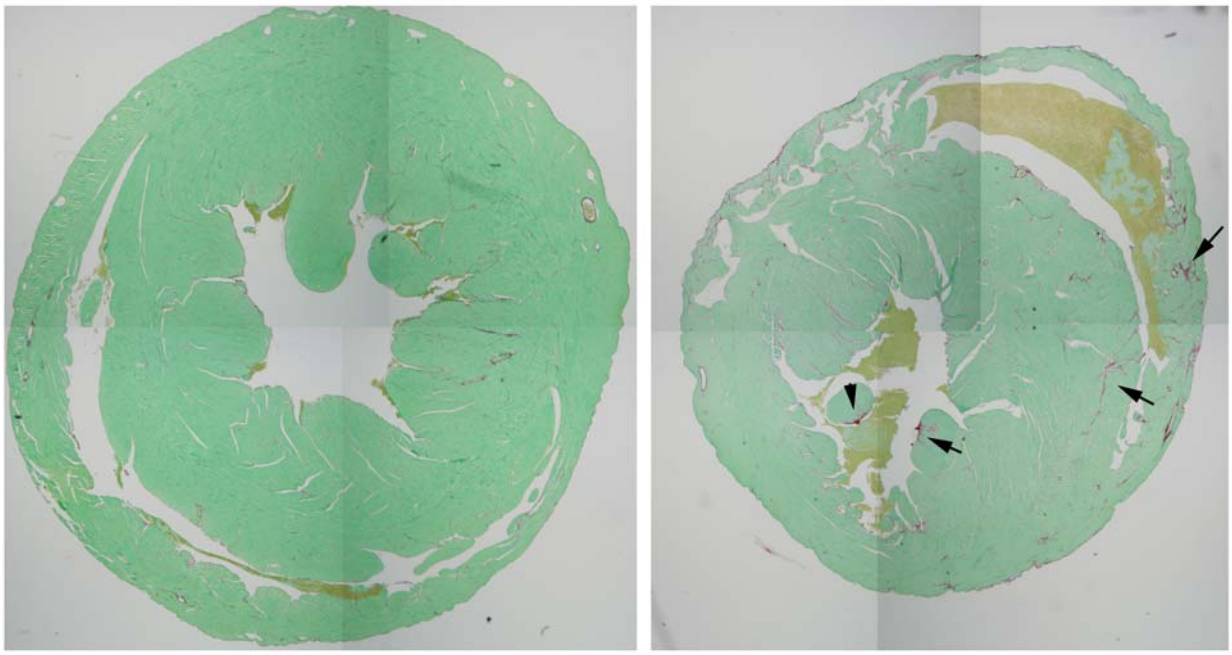

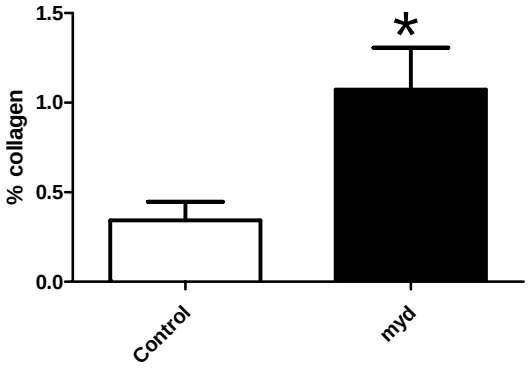

Supplemental Figure 4. Representative entire cross sections of myocardium from *myd* mice and littermate control mice at 50 weeks of age. Focal deposition of interstitial collagen is observed in both left and right ventricles (arrows) of myd mice, but overall the phenotype appears milder than that observed in 50 week old MLC2vcre-L/L mice (shown in figure 3). Image analysis indicted the total area of collagen deposition was significantly increased in *myd* mice compared to littermate control mice (data are mean +/- SEM, *=$p<0.05$, n=3). While some perivascular collagen is observed in both WT and myd animals, the increase observed in collagen in myd animals is primarily due to increase in interstitial collagen.

REFERENCES FOR SUPPLEMENT

1. Moore, S.A., Saito, F., Chen, J., Michele, D.E., Henry, M.D., Messing, A., Cohn, R.D., Ross-Barta, S.E., Westra, S., Williamson, R.A., et al. 2002. Deletion of brain dystroglycan recapitulates aspects of congenital muscular dystrophy. *Nature* 418:422-425.
2. Chen, J., Kubalak, S.W., and Chien, K.R. 1998. Ventricular muscle-restricted targeting of the RXRalpha gene reveals a non-cell-autonomous requirement in cardiac chamber morphogenesis. *Development* 125:1943-1949.
3. Regan, C.P., Manabe, I., and Owens, G.K. 2000. Development of a smooth muscle-targeted cre recombinase mouse reveals novel insights regarding smooth muscle myosin heavy chain promoter regulation. *Circ Res* 87:363-369.
4. Michele, D.E., Barresi, R., Kanagawa, M., Saito, F., Cohn, R.D., Satz, J.S., Dollar, J., Nishino, I., Kelley, R.I., Somer, H., et al. 2002. Post-translational disruption of dystroglycan-ligand interactions in congenital muscular dystrophies. *Nature* 418:417-422.
5. Weiss, R.M., Ohashi, M., Miller, J.D., Young, S.G., and Heistad, D.D. 2006. Calcific aortic valve stenosis in old hypercholesterolemic mice. *Circulation* 114:2065-2069.
6. Hill, J.A., Karimi, M., Kutschke, W., Davisson, R.L., Zimmerman, K., Wang, Z., Kerber, R.E., and Weiss, R.M. 2000. Cardiac hypertrophy is not a required compensatory response to short-term pressure overload. *Circulation* 101:2863-2869.
7. Gaussin, V., Tomlinson, J.E., Depre, C., Engelhardt, S., Antos, C.L., Takagi, G., Hein, L., Topper, J.N., Liggett, S.B., Olson, E.N., et al. 2003. Common genomic response in different mouse models of beta-adrenergic-induced cardiomyopathy. *Circulation* 108:2926-2933.
8. Mahoney, D.J., Carey, K., Fu, M.H., Snow, R., Cameron-Smith, D., Parise, G., and Tarnopolsky, M.A. 2004. Real-time RT-PCR analysis of housekeeping genes in human skeletal muscle following acute exercise. *Physiol Genomics* 18:226-231.
9. Lupberger, J., Kreuzer, K.A., Baskaynak, G., Peters, U.R., le Coutre, P., and Schmidt, C.A. 2002. Quantitative analysis of beta-actin, beta-2-microglobulin and porphobilinogen deaminase mRNA and their comparison as control transcripts for RT-PCR. *Mol Cell Probes* 16:25-30.
10. Kuhn, M., Voss, M., Mitko, D., Stypmann, J., Schmid, C., Kawaguchi, N., Grabellus, F., and Baba, H.A. 2004. Left ventricular assist device support reverses altered cardiac expression and function of natriuretic peptides and receptors in end-stage heart failure. *Cardiovasc Res* 64:308-314.
11. Livak, K.J., and Schmittgen, T.D. 2001. Analysis of relative gene expression data using real-time quantitative PCR and the 2(-Delta Delta C(T)) Method. *Methods* 25:402-408.
12. Grewal, P.K., McLaughlan, J.M., Moore, C.J., Browning, C.A., and Hewitt, J.E. 2005. Characterization of the LARGE family of putative glycosyltransferases associated with dystroglycanopathies. Glycobiology 15:912-923.
13. Kurahashi, H., Taniguchi, M., Meno, C., Taniguchi, Y., Takeda, S., Horie, M., Otani, H., and Toda, T. 2005. Basement membrane fragility underlies embryonic lethality in fukutin-null mice. Neurobiol Dis 19:208-217.
14. Willer, T., Prados, B., Falcon-Perez, J.M., Renner-Muller, I., Przemeck, G.K., Lommel, M., Coloma, A., Valero, M.C., de Angelis, M.H., Tanner, W., et al. 2004. Targeted disruption of the Walker-Warburg syndrome gene Pomt1 in mouse results in embryonic lethality. Proc Natl Acad Sci U S A 101:14126-14131.
15. Williamson, R.A., Henry, M.D., Daniels, K.J., Hrstka, R.F., Lee, J.C., Sunada, Y., Ibraghimov-Beskrovnaya, O., and Campbell, K.P. 1997. Dystroglycan is essential for early embryonic development: disruption of Reichert's membrane in Dag1-null mice. Human Molecular Genetics 6:831-841.